Automated Laser Beam Characterizer

Zachary Andreasen, Thomas Cunningham, and Lynzie Smith

Dept. of Electrical Engineering and Computer Science, University of Central Florida, Orlando, Florida, 32816-2450

***Abstract* – In any lab that seeks to use a laser, it is critical to know the many of the exact properties of the laser to know precisely how it will behave. This project aims to automate the process of measuring basic laser characteristics, thereby streamlining the process of data collection and lab experimentation. The designed system characterizes a laser's polarization, wavelength, beam quality (M^2 Factor), and divergence. The system accommodates a broad range of input powers and wavelengths, allowing for flexible use in many different lab environments.**

***Index Terms* – Polarimeter, M^2 Factor, Interferometry, Laser**

I. Introduction

Optical experiments all rely on knowing key parameters about your laser beam. When these parameters are not known, there is little to do before obtaining them. This process can take hours to perform by hand, and the process takes away from valuable lab hours.

This project seeks to take the hassle out of characterizing your laser beam; by automating the full process, the engineer can use that time in a more productive way. But this is only possible if he trusts the system to give accurate results. The system is designed to provide the most accurate and consistent high-level measurements for the most fundamental laser beam characteristics.

This project is aimed at lasers in the near-infrared region, spanning 1-2 µm wavelengths, making it useful for many different systems. Additionally, the system will accommodate a large range of input beam sizes and optical powers. These specifications for shown in the table below.

TABLE 1
SYSTEM INPUT SPECIFICATIONS

Parameter	Value	Units
Wavelength	1-2	µm
Input Power	0.01 – 10	W
Beam Size	4 - 35	mm

II. Optical Design

A. Polarization

To measure the polarization of the laser beam, the rotating quarter waveplate method is employed to uniquely measure the four Stokes parameters, shown below.

$$S = \begin{pmatrix} S_0 \\ S_1 \\ S_2 \\ S_3 \end{pmatrix} \tag{1}$$

As described in an article published in the American Journal of Physics, "the parameter S_0 describes the total intensity of the optical field, S_1 describes the preponderance of linearly horizontally polarized light (LHP) over linearly vertically polarized light (LVP), S_2 describes the preponderance of linear +45° polarized light (L +45P) over linear −45° polarized light (L−45P), and the fourth parameter S_3 describes the preponderance of right circularly polarized light (RCP) over left circularly polarized light (LCP)". [1] The determination of these parameters allows the system to determine the lasers position on the Poincare sphere and plot the polarization ellipse.[2] [3]The rotating quarter waveplate method consists of three components in the following order: a quarter waveplate, a linear polarizer, and a power meter. The image below shows the general setup of this method.

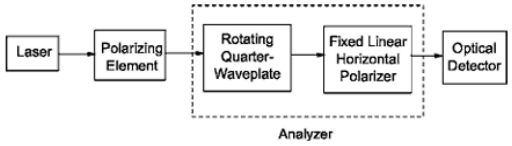

Fig. 1. Diagram of Components for a Polarimeter using the Rotating Quarter Waveplate method. Moving from left to right, there is the laser, which is polarized in some way by the polarizing element. The actual polarimeter follows this, consisting of the analyzer (Quarter Waveplate and Linear Polarizer) followed by the detector which will measure the optical power as a function of Quarter Waveplate angle [1]

The power read by the power meter will be affected by the angle of the quarter waveplate and the linear polarizer. By keeping the linear polarizer fixed and rotating the quarter waveplate, the power transmitted through the linear polarizer can be written as a linear combination of the original four Stokes parameters, whose coefficients are determined only by the angle of the quarter waveplate with respect to the transmission axis of the linear polarizer, shown below. [1]

$$I(\theta) = \frac{1}{2}[S_0 + S_1\cos^2(\theta) + S_2\cos(2\theta)\sin(2\theta) + S_3\sin(2\theta)] \tag{2}$$

Therefore, using this method, the system derives the four Stokes parameters from which the polarization ellipse can be plotted. [4] This is useful since in many applications the

polarization of the laser beam affects its behavior in an optical setup.

B. M^2 Factor and Divergence

The measurement of the laser beam's M^2 Factor and Divergence are grouped into one section because of the similarity with which the data is collected. In both cases, the system obtains an intensity profile of the beam and determines the approximate beam width by performing a knife edge test, where a thin blade is scanned across the path of the beam and the power curve is read. The derivative of this power curve is equal to the actual intensity profile of the beam. To save resources, the same power meter used in the polarimeter is reused in this subsystem.

For the M^2 factor measurement, it is necessary to simultaneously know the divergence and beam waist of the laser, done by determining the size of the beam at several points within the Rayleigh range and several points outside the Rayleigh range. As most lasers are collimated and have a very long Rayleigh range, this is not feasible without focusing the lens and determining the new divergence and beam waist of the focused beam.

To ensure the measurements are accurate, ISO 11146 Standard specifies the ideal data collection procedures. There are two main specifications that are relevant. The first is the definition of the beam width. There are many ways in which the width of the beam can be described (FWHM, $1/e^2$, etc.). The ISO Standard specifies that the D4σ width should be used. This defines the diameter of the beam to be 4 times the standard deviation of the intensity distribution curve extracted from the knife edge scan. Additionally, there are specifications for where along the path of the beams propagation the profiles must be taken. The ISO Standard specifies that at least 5 points must be taken within one Rayleigh range and at least 5 points must be taken outside two Rayleigh ranges. [5] These standards limit how long the focal length of the lens used must be and how long the system must scan to be able to measure all the correct points. To accomplish this, the system uses an 812 mm focal length lens, and scans across an effective length of 600 mm.

For the Divergence measurement, as mentioned above, it is not feasible to profile the beam at several points as this would require scanning a long distance. Using the same lens as the used for M^2 Factor measurement, the width of the beam at the focal point of the lens can be measured. Using simple ray tracing techniques, the divergence of the beam prior to the lens can be determined from the following equation: [6]

$$\theta = \frac{w}{f} \tag{3}$$

Where θ is the divergence of the beam prior to the lens, w is the width of the beam at the focal length of the lens, and f is the focal length of the lens. In this way, the system measures the divergence of the beam.

C. Wavelength

The wavelength measurement is not only an important property to know for the laser beam but is also important for the rest of the measurements performed in the system. For example, the retardance of the quarter waveplate used in the polarimeter is wavelength dependent and therefore will affect the Stokes parameters measurement. Additionally, the focal length of the lens in the system as well as the calculation of the M^2 factor is dependent on the wavelength of the laser. For this reason, the wavelength measurement is performed first before all the measurements explained above. This will allow for the proper corrections to be made to the other measurements to ensure their accuracy.

The wavelength measurement is taken using a Michelson Interferometer. One mirror in the interferometer is moved, and the interference pattern is be read. In many interferometer setups, the number of peaks traversed for a certain mirror displacement is used to calculate the wavelength using Equation 4 below. However, due to the lack of a sufficiently small step size and potential noise factors which can distort this measurement, this system does not use this method but rather moves the mirror at a constant speed and samples the signal using a photodiode sensor, described below. The frequency of this signal is related to the wavelength of the laser beam as shown in Equation 5 below, derived by taking the derivative with respect to time of Equation 4.

$$m\lambda = 2\Delta x \tag{4}$$

$$\lambda = \frac{2\mathrm{v}}{\mathrm{f}} \tag{5}$$

Where λ is the wavelength of the laser beam (m), Δx is the mirror displacement (m), m is the number of peaks of the signal passed through a certain point for the same mirror displacement (unitless), v is the speed of the mirror moved (m/s), and f is the frequency of the interference signal created by moving the mirror (Hz).

D. Full System Setup

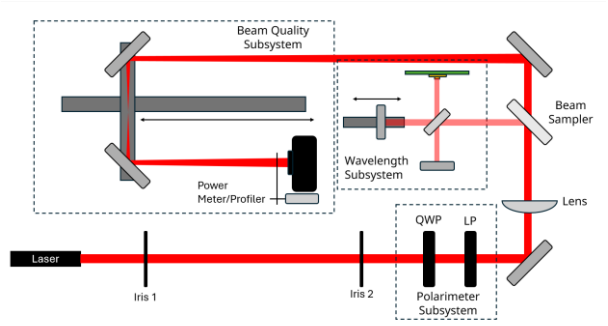

Fig. 2. Layout of all optical hardware. At the bottom can be seen the two irises the used must align the laser, after which it immediately moves into the polarimeter subsystem. After this it travels through the focusing lens and a small portion of the beam is split off to go into the interferometer for wavelength measurement. Finally, the beam is directed into the beam quality subsystem where a scanning slit will profile the beam at different points along the beams focused path for M^2 Factor and Divergence measurement.

Above is the full layout of all the optical components of the three subsystems described in the preceding sections. Putting these subsystems together requires careful optical design planning. There are many factors that must be considered to ensure the system functionality, including optical power, input beam size, and alignment tolerance. To minimize misalignments into the system, two irises are set up at the input to the system spaced 16 inches apart. The user will need to align the laser to these irises as close as possible to ensure the system can take all the necessary measurements. Additionally, to accommodate the large beam size specification, at least 2-inch diameter optics needed to be used to not clip the beam. Also, to not oversaturate the sensors used in the system, appropriate power attenuation must be employed to meet the required power specifications. There are three main methods in which the system accomplishes this. The first is the use of ND Filters. These are implemented at the input of the system as well as over the photodiode used to measure wavelength. By making these filters movable, the system can accommodate large as well as small input powers. The second is the power meter selected to be used for the polarimeter, M^2 factor, and divergence measurements. The system uses the S148C power meter head available from Thor Labs. This power meter uses a photodiode embedded in an integrating sphere, which gives it a low responsivity. This allows the higher powers lasers to be read without the need for significant optical attenuation. Lastly is the use of a beam sampler to pick off a small portion of the laser signal to use in the Michelson interferometer. This will allow for a photodiode to read the high-power signals without oversaturating the sensor.

III. Electrical Hardware

A. Microcontroller

The microcontroller for this system has the task of controlling the motors, reading sensors, and streaming the data back to a personal computer for processing. It is critical that the microcontroller can handle all the motors in the system with precision and consistency. The STM32G474 is an industry standard for robust, hardware-driven microcontrollers.

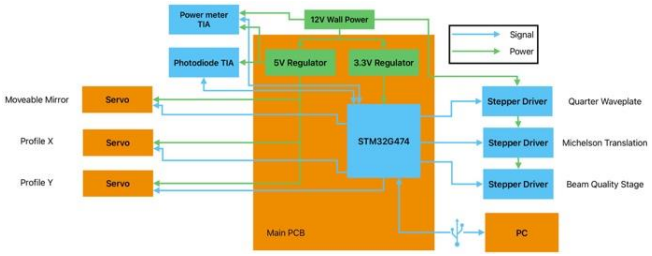

Fig. 3. General overview of STM32 interface

B. Motors

Motors play a critical role in making sure the systems run smoothly and accurately, so it is important to use the correct motors in each step. There were shortcomings in the initial selection, and updates are currently being made to solve the issues we are having.

Stepper motors are used for two main applications: ball screw translation stages and belt driven rotation. They provide very precise angle control. Due to the relatively light load, we can use small motors.

The translation application uses a prebuilt CNC system with a NEMA 13 motor already integrated. This allows us to focus on the measurement protocol instead of designing our own translation stage.

For the belt driven rotation, we design a custom 3D printed system to reliably rotate the quarter wave plate in the system. The rig provides a 1:4 gear reduction to the stepper motor's rotation, providing even more precision to the system.

Fig. 4. Custom belt driven quarter waveplate rotator

The stepper motors are driven by a DRV8825 stepper motor driver from Texas Instruments. The circuit based on the application from the datasheet, allowing for a flexible voltage input from 12V to 24V. The pins are ordered the same order as commercially available stepper motor drivers with the same chip for compatibility.

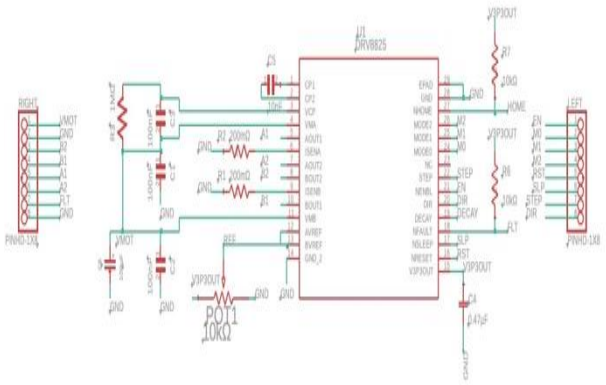

Fig. 5. DRV8825 application schematic

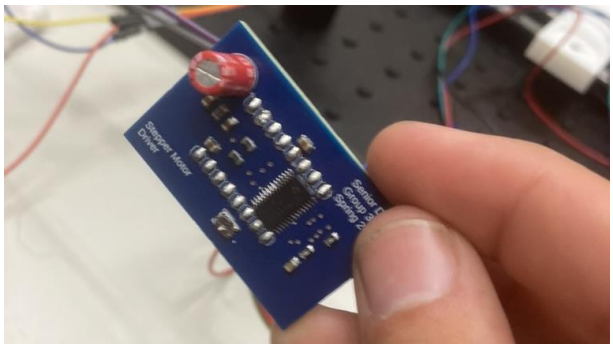

Fig. 6. DRV8825 pin swappable PCB

For the beam profiling, we planned on using servo motors to scan, but they did not have enough resolution, and the test scans were not consistent across runs. The current fix to this is to use geared brushed DC motors with an encoder to scan the beam at constant velocity. This changes the scanning method from incremental to continuous scanning and should increase the accuracy in the measurements.

C. Photodiode Sensors

There are two photodiode sensors that are used in this system. The first is the Thor Labs S148C Power Meter Head. As mentioned above, this detector is embedded in an integrating sphere, which gives it a low responsivity. This photodiode is used in the polarization, M^2 Factor, and Divergence measurements. Because the rotation of the quarter waveplate as well as the knife edge scans require both the high and low power measurements, a transimpedance amplifier was used with a variable gain, achieved by putting a multiplexor chip in the feedback loop so that the feedback resistance can be changed based on which line in the multiplexor is active. The schematic for this is shown below.

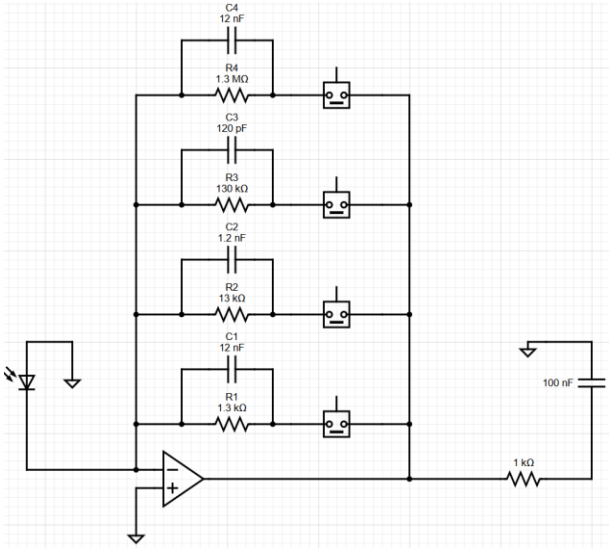

Fig. 7. Variable Gain Transimpedance Amplifier Schematic. In order from top to bottom, the gain resistors are 1.3 kΩ, 13kΩ, 130kΩ, and 1.3MΩ. Each is tied to a digital switch that will change which resistors contribute to the gain of the amplifier. This is designed so each gain state has 10X gain of the previous state. Each gain state has its own feedback capacitance to help with stability. In the same order, they are 12nF, 1.2nF, 120pF, and 12pF. There is also a low pass filter at the output to filter out noise.

The second photodiode used is an extended InGaAs photodiode and is used to read the signal from the Michelson Interferometer. Since the speed of the mirror can easily be controlled, the motor is set to move the mirror at 10 mm/s. This will create a 50 kHz signal at 1 µm wavelength and a 25 kHz signal at 2 µm wavelength. This is well within achievable bandwidth for the photodiode

sensor to read the signal and determine its frequency. The schematic for this is shown below.

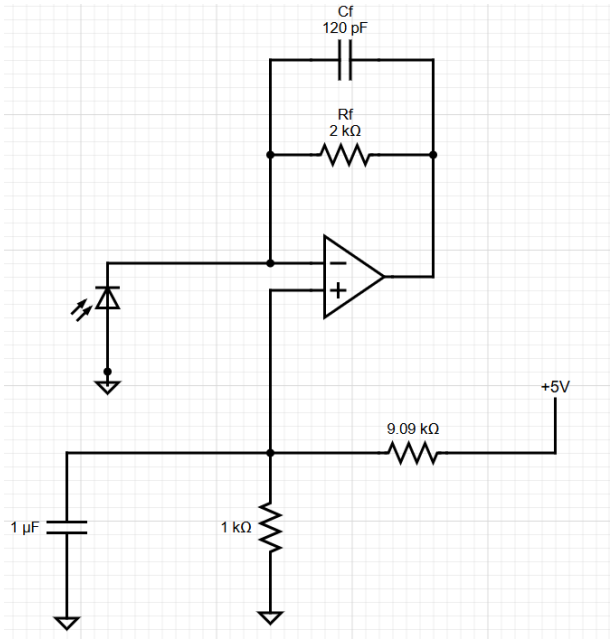

Fig. 8. Schematic of Transimpedance Amplifier used to read the interference pattern created by moving one mirror in the Michelson Interferometer.

IV. Software

The software system is designed to support real-time laser beam characterization through coordinated control, data acquisition, and analysis. A dual-layer architecture is implemented, consisting of embedded firmware for deterministic measurement execution and a host-based graphical user interface (GUI) for computation, visualization, and user interaction. Communication between layers is achieved via a USB CDC interface using structured packet exchange.

A. *System Architecture*

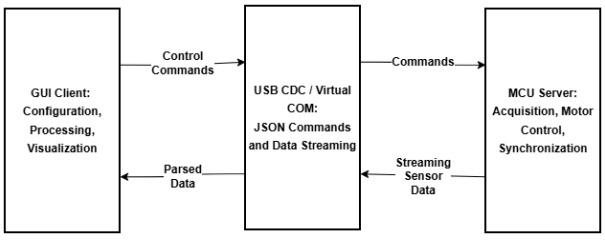

Fig. 9. Software system architecture showing the host GUI as client and microcontroller as real-time data server communicating with USB CDC interface.

The overall system follows a client-server model in which the microcontroller operates as a real-time data server, while the GUI functions as an analytical client. The firmware is responsible for time-critical operations including analog data acquisition, motor actuation, and synchronization of optical components. The GUI manages experiment configurations, streaming data processing, and visualization.

Communication occurs over a virtual COM port using lightweight JSON-formatted messages containing timestamps, sensor readings, and control commands. The system is designed for asynchronous operation, allowing continuous data streaming from the microcontroller while the GUI simultaneously issues commands and updates visual outputs.

B. *Embedded Firmware Design*

The embedded firmware is implemented in C and structured using a modular design paradigm. Core functional modules include sensor acquisition, motor control, and communication handling, each encapsulated in independent source files. This modularity improves maintainability and enables isolated subsystem testing.

Real-time performance is achieved using a multitasking architecture under a real-time operating system. Time-critical processes such as ADC sampling and actuator control are driven by hardware timers and interrupts, ensuring deterministic execution. Data is temporarily stored in circular buffers to prevent overflow during high-rate acquisition before transferring to the host computer.

Peripheral interfacing is handled through a 12-bit ADC for photodiode signal acquisition and a USB CDC interface for communication with the host computer, and pulse-driven GPIO or PWM outputs for motor control and positioning of optical components.

A command-response protocol enables flexible control, where the firmware parses incoming JSON commands and streams measurement data accordingly. A watchdog timer ensures system reliability by resetting the microcontroller in the event of task failure or deadlock.

C. *GUI Application Design*

The host application is implemented in Python using PySide6 and follows a Model-View-Controller (MVC) architecture. This structure separates data processing, user interface, and control logic to improve scalability and maintainability. The Model component manages data buffering, numerical computations, and metric extraction, including operations such as FFT analysis, curve fitting, and Stokes parameter estimation. The View is responsible for real-time visualization using Qt widgets and Matplotlib plots to display measurement data and system status. The Controller mediates between user inputs and system behavior by translating interface actions into commands and managing communication with the firmware.

Asynchronous timers are used to update plots without blocking the main event loop, ensuring smooth visualization during continuous data acquisition. A dedicated communication class manages serial I/O, buffering, and error handling.

D. Subsystem Integration

Integration between firmware and GUI was achieved through a USB CDC interface that emulates a serial connection. Data packets follow a structured format consisting of a header, JSON payload, and checksum to ensure integrity.

The GUI continuously listens for incoming messages using non-blocking I/O, allowing for concurrent visualization and command execution. This architecture enables seamless switching between simulation and hardware operation without modifying the processing pipeline.

E. System Operation

Upon application startup, the GUI initializes its interface, data buffers, and communication handlers, then attempts to establish a connection with the microcontroller over the USB CDC virtual COM interface. If a valid connection is detected, the system will remain in an idle state, awaiting user input.

The user is allowed to select a desired measurement mode, which triggers the corresponding configuration sequence. Control commands are transmitted from the GUI to the microcontroller, where the firmware configures the necessary peripherals, including ADC sampling, motor control, and synchronization of optical components.

During operation, the microcontroller continuously acquires sensor data and streams measurement packets to the GUI in real time. These packets include timestamps, raw sensor values, and status information. The GUI processes incoming data asynchronously, updating plots, computing intermediate metrics, and providing immediate visual feedback without interrupting the ongoing acquisition.

Once the measurement sequence is complete, the GUI performs final computations and presents the results to the user. The system then returns to the idle state, ready for subsequent measurements. This operational design ensures continuous data flow, responsive user interaction, and consistent behavior.

V. Summary

In summary, this need for accurate and convenient acquisition of data concerning basic laser characteristics can be easily met using this system. It not only measures the wavelength, polarization, M^2 Factor, and the divergence of the beam, but also does so in an automated and efficient manner. By incorporating several different motors into the system, the process of data collection becomes quick and easy, freeing up useful lab time and energy. The system is also designed in such a way that it is useful in many different lab environments. From wavelengths of 1 to 2 microns, powers from as low as 10 mW to as high as 10 W, and from beam sizes as small as 4 mm to as large as 35 mm, this system can accomplish its objectives and see to it that the beam is fully characterized in its most basic characteristics.

Engineers

Zachary Andreasen is a 22-year-old Electrical and Photonics Science Engineering student. He is taking a job after graduation at Lockheed Martin working in Electro-Optics.

Thomas Cunningham is an aspiring Electrical Engineer who loves to get his hands dirty with hardware and think deeply about solving complex problems.

Lynzie Smith is a Computer Engineering student who wants to pursue a career working with embedded systems after graduation.

Acknowledgements

The authors wish to acknowledge the assistance of Lockheed Martin Special Programs for sponsoring this project, with special thanks to James (Cooper) Reid for his assistance in ordering hardware.

References

[1] B. Schaefer, E. Collett, R. Smyth, D. Barrett, and B. Fraher, "Measuring the Stokes polarization parameters," *Am. J. Phys.*, vol. 75, no. 2, pp. 163–168, Feb. 2007, doi: 10.1119/1.2386162.

[2] "Using the Poincaré Sphere to Represent the Polarization State." [Online]. Available:

https://www.thorlabs.com/newgrouppage9.cfm?objectgroup_id=14200
[3] "The Polarization Ellipse Representation of the Polarization State." [Online]. Available: https://www.thorlabs.com/newgrouppage9.cfm?objectgroup_id=14199
[4] Thorlabs, *Build a Polarimeter to Find Stokes Values, Polarization State (Viewer Inspired) | Thorlabs Insights*, (Oct. 20, 2021). [Online Video]. Available: https://youtu.be/pR4r7gMyN5U
[5] R. Paschotta, "M^2 factor – M squared, laser beam, quality factor, beam divergence, caustic, ISO Standard 11146." Accessed: Sep. 05, 2025. [Online]. Available: https://www.rp-photonics.com/m2_factor.html
[6] Litron Lasers, "Comparison of Beam Divergence, Beam Diameter and M2," 2025, [Online]. Available: https://www.litronlasers.com/technical-notes/comparison-of-beam-divergence-beam-diameter-m2/